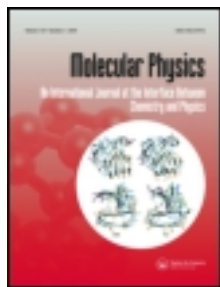


This article was downloaded by: [Mohit Swadia]

On: 12 June 2013, At: 10:11

Publisher: Taylor & Francis

Informa Ltd Registered in England and Wales Registered Number: 1072954 Registered office: Mortimer House, 37-41 Mortimer Street, London W1T 3JH, UK



Molecular Physics: An International Journal at the Interface Between Chemistry and Physics

Publication details, including instructions for authors and subscription information:

<http://www.tandfonline.com/loi/tmph20>

Electron impact total cross section calculations for CH₃SH (methanethiol) from threshold to 5 keV

Chetan Limbachiya^a, Minaxi Vinodkumar^b, Mohit Swadia^a & Avani Barot^b

^a P.S. Science & H.D. Patel Arts College, Kadi, Gujarat, 382715, India

^b V P & R P T P Science College, Vallabh Vidyanagar, Gujarat, 388120, India

Accepted author version posted online: 03 May 2013. Published online: 11 Jun 2013.

To cite this article: Chetan Limbachiya, Minaxi Vinodkumar, Mohit Swadia & Avani Barot (2013): Electron impact total cross section calculations for CH₃SH (methanethiol) from threshold to 5 keV, *Molecular Physics: An International Journal at the Interface Between Chemistry and Physics*, DOI:10.1080/00268976.2013.802038

To link to this article: <http://dx.doi.org/10.1080/00268976.2013.802038>

PLEASE SCROLL DOWN FOR ARTICLE

Full terms and conditions of use: <http://www.tandfonline.com/page/terms-and-conditions>

This article may be used for research, teaching, and private study purposes. Any substantial or systematic reproduction, redistribution, reselling, loan, sub-licensing, systematic supply, or distribution in any form to anyone is expressly forbidden.

The publisher does not give any warranty express or implied or make any representation that the contents will be complete or accurate or up to date. The accuracy of any instructions, formulae, and drug doses should be independently verified with primary sources. The publisher shall not be liable for any loss, actions, claims, proceedings, demand, or costs or damages whatsoever or howsoever caused arising directly or indirectly in connection with or arising out of the use of this material.

Electron impact total cross section calculations for CH₃SH (methanethiol) from threshold to 5 keV

Chetan Limbachiya^{a,*}, Minaxi Vinodkumar^b, Mohit Swadia^a and Avani Barot^b

^aP.S. Science & H.D. Patel Arts College, Kadi-382 715, Gujarat, India; ^bV P & R P T P Science College, Vallabh Vidyanagar-388 120, Gujarat, India

(Received 12 March 2013; final version received 27 April 2013)

We report calculated total elastic cross sections Q_{el} , total ionisation cross sections, Q_{ion} , summed total excitation cross sections $\sum Q_{exc}$ and total cross sections Q_T for CH₃SH upon electron impact for energies from ionisation threshold to 5 keV. We have employed Spherical Complex Optical Potential (SCOP) formalism to calculate total elastic cross section Q_{el} , and total inelastic cross section Q_{inel} and used Complex Scattering Potential – the ionisation contribution (CSP-ic) method to extract the ionisation cross sections, Q_{ion} , from the calculated Q_{inel} . The calculated total cross sections are examined as functions of incident electron energy and are compared with available data wherever possible and overall good agreement is observed. In this work Q_{el} , Q_{ion} , and $\sum Q_{exc}$ are reported for the first time for CH₃SH in this energy range.

Keywords: spherical complex optical potential (SCOP); complex scattering potential – ionisation contribution (CSP-ic); total ionisation and total cross sections; CH₃SH

I. Introduction

Electron interactions with molecules play an important role in exploring various physico-chemical phenomena occurring in chemical as well as biological environments. A study of electron-driven processes is useful for various applied sciences and reflects the fundamental structural properties of the investigated target. Total cross sections for the ionisation and excitation of atoms and molecules by electron impact is one of the essential sets of data needed in a wide range of applications, such as modelling plasmas for plasma processing of semiconductors, designing mercury-free fluorescent lamps, assessing the efficiency of ion gauges, normalising mass spectrometer output, diagnosing plasmas in magnetic fusion devices, and modelling radiation effects on materials.

Methanethiol (CH₃SH), abbreviated as MeSH is a colourless weak acid found in the blood and brain of humans and other animal as well as plant tissues. At a very high concentration it is highly toxic and affects the central nervous system. Electron-driven processes on CH₃SH find applications in chemical industry as well as in the field of biochemistry. It is one of the most important products of degradation of organic matter, and interesting in view of its presence in the Earth's atmosphere and in interstellar space [1]. Methanethiol is mainly used to produce methionine, which is used as a dietary component in poultry and animal feed [2]. Despite wide applications and the importance

of electron-driven processes on CH₃SH, the molecule is less explored. The only information about electron interaction with methanethiol is available from the experiments of non-local dissociation by Maksymovych *et al.* [3], dissociative attachment by Jäger and Henglein [4], investigations of positive-ion formation by Amos *et al.* [5] and the lower energy (0–7 eV) transmission measurements of Dezarnaud *et al.* [6].

The objective of the present work is to supplement hitherto sparse electron impact cross section data for CH₃SH in the intermediate energy range from threshold to 5 keV. While Szymtkowski *et al.* [7] have measured total (complete) cross sections, total ionisation and total elastic cross sections for CH₃SH have not been reported. We report here various total cross sections for CH₃SH on electron impact for energies from threshold to 5000 eV.

Figure 1 shows the geometry of methanethiol and the basic properties of the molecule are given in Table 1.

In the present calculation we compute total cross sections (TCS) using group additivity. The groups, which are used to calculate TCS for CH₃SH, are CH₃ and SH. Such a choice emerges from the geometry of the molecule and larger C–S bond length as compared to C–H and S–H bond lengths. Due to large C–S bond length, the CH₃ and SH can be treated as separate groups and the cross sections are calculated for these groups and summed to get the total cross sections.

*Corresponding author. Email: chetanlimbachiya2@yahoo.com

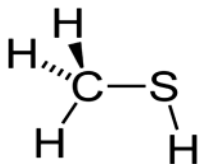


Figure 1. Geometry of methanethiol. $\angle\text{HSC} = 96.5^\circ$ and $\angle\text{HCH} = 109.8^\circ$ [31].

II. Theoretical methodology

In order to calculate the total cross sections, we have employed spherical complex optical potential (SCOP) formalism [8–11] through which the total elastic cross sections Q_{el} and inelastic cross sections Q_{inel} are obtained such that,

$$Q_T(E_i) = Q_{el}(E_i) + Q_{inel}(E_i). \quad (1)$$

The electron-molecule interaction can be represented by a complex potential,

$$V(r, E_i) = V_R(r, E_i) + iV_I(r, E_i), \quad (2)$$

where, $V_R(r, E_i)$ is the real potential term and $V_I(r, E_i)$ is an imaginary potential term that represents the absorption potential.

Here,

$$V_R(r, E_i) = V_{st}(r) + V_{ex}(r, E_i) + V_{pol}(r, E_i). \quad (3)$$

The three terms on the RHS of Equation (3) represent various real potentials viz. static, exchange and polarisation potentials that arise due to electron target interactions. To evaluate all these potentials, the most basic input is the charge density of the target. The spherically averaged charge density $\rho(r)$ of the molecule and static potential $V_{st}(r)$ are determined from the constituent atomic charge densities derived from the Hartree–Fock wave functions given by Cox and Bonham [12].

The static potential of the target is a characteristic potential described by the charge density of each atom in the molecule. The static potential $V_{st}(r)$ is the potential experienced by the incident electron upon approaching the field of an unperturbed target charge cloud. The static potential is calculated at the Hartree–Fock level using fixed nuclei approximation [9]. For the exchange potential, we have employed Hara’s free electron gas exchange model [13], which

is parameter-free and energy-dependent. For the polarisation potential V_{pol} , we have used a parameter-free model of correlation potential by Zhang *et al.* [14]. Here, various multipole non-adiabatic corrections are incorporated in the intermediate region that will approach the correct asymptotic form at the large ‘ r ’ smoothly.

The imaginary part V_I of the complex potential in Equation (2) contains absorption potential, which represents the effects of all inelastic channels. Here we have employed a well-known non-empirical quasi-free model form given by Staszewska *et al.* [15] as given below.

$$\begin{aligned} V_{abs}(r, E_i) &= -\rho(r) \sqrt{\frac{T_{loc}}{2}} \left(\frac{8\pi}{10k_f^3 E_i} \right) \times \theta(P^2 - k_F^3 - 2\Delta) \\ &\quad \times (A_1 + A_2 + A_3) \end{aligned} \quad (4)$$

The local kinetic energy of the incident electron is $T_{loc} = E_i - (V_{st} + V_{ex})$.

The parameters A_1 , A_2 , and A_3 in Equation (4) are given as,

$$\begin{aligned} A_1 &= 5 \frac{k_f^3}{2\Delta}, \quad A_2 = \frac{k_f^2 (5p^2 - 3k_f^2)}{(5p^2 - 3k_f^2)} \text{ and} \\ A_3 &= \frac{2\theta(2k_f^2 + 2\Delta - p^2) (2k_f^2 + 2\Delta - p^2)^{5/2}}{(p^2 - k_f^2)^2}. \end{aligned}$$

The absorption potential is not sensitive to long-range interactions like V_{pol} . In Equation (4), $p^2 = 2E_i$, $k_F = [3\pi^3 \rho(r)]^{1/3}$ is the Fermi wave vector and Δ is an energy parameter. Further $\theta(X)$ is the Heaviside unit step-function, such that $\theta(X) = 1$ for $X \geq 0$ and is zero otherwise. The dynamic functions A_1 , A_2 and A_3 occurring in Equation (4) depend differently on $\theta(X)$, I , Δ and E_i , where I is the ionisation threshold of the target. The energy parameter Δ determines a threshold below which $V_{abs} = 0$, and the ionisation or excitation is prevented energetically. In fact Δ is the governing factor that decides the value of the total inelastic cross sections and that is one of the characteristics of the Staszewska model [15]. We have modified the original model by considering Δ as a slowly varying function of E_i around I in order to incorporate the inelastic processes occurring even below the ionisation potential viz. excitation processes [16–19]. Further Δ as a variable, accounts for the screening of the absorption potential in the target charge-cloud region as suggested by Blanco and Garcia [20]. This is meaningful since Δ fixed at I would not allow excitation at incident energy $E_i \leq I$. On the other hand, if the parameter Δ is much less than the ionisation threshold, then V_{abs} becomes exceedingly high near the peak position. The modification introduced in our paper is aimed at assigning

Table 1. Properties of CH_3SH .

Ionisation potential (eV) [31]	Dipole moment (Debye) [31]	Bond lengths (Å) [31]	Polarisability (Å ³) [32]
9.44	1.52	C–H 1.09 C–S 1.819 S–H 1.34	5.31

a reasonable minimum value $0.8I$ to Δ and express this parameter as a function of E_i around I as follows [21].

$$\Delta(E_i) = 0.8I + \beta(E_i - I) \quad (5)$$

In Equation (5) β is obtained by requiring that $\Delta = I$ (eV) at $E_i = E_p$, beyond which Δ is held constant and equal to I . Here E_p is the value of incident energy at which our Q_{inel} reaches its peak. After generating the full complex potential given in Equation (2), we solve the Schrodinger equation numerically using partial wave analysis to obtain complex phase shifts. In the low-energy region, the small 'r' region is not important due to the fact that higher-order partial waves are unable to penetrate the scattering region. However in the present energy region, a large number of partial waves contribute to the scattering parameters and correct short-range behaviour of the potential is essential. These complex phase shifts that carry the signature of electron target interactions are employed in the standard formulae to find the cross section given in Equation (1).

The total inelastic cross sections, Q_{inel} cannot be measured directly in experiments. The measurable quantity of applied interest is the total ionisation cross sections, Q_{ion} , which is contained in the Q_{inel} . The Q_{inel} can be partitioned into discrete and continuum contributions, viz.

$$Q_{inel}(E_i) = \sum Q_{exc}(E_i) + Q_{ion}(E_i), \quad (6)$$

where, the first term is the summed total excitation cross sections for all accessible electronic transitions. The second term is the total cross sections of all allowed ionisation transitions to a continuum induced by the incident electrons. The first term arises mainly from the low-lying dipole allowed transitions for which the cross section decreases rapidly at higher energies. The first term in Equation (6), therefore becomes progressively smaller than the second at energies well above the ionisation threshold. By definition,

$$Q_{inel}(E_i) \geq Q_{ion}(E_i). \quad (7)$$

This is an important inequality and forms the basis of our method of extraction of Q_{ion} from Q_{inel} . This method is called Complex Scattering Potential-ionisation contribution (CSP-ic) [22,23]. We define the following energy dependent ratio of cross sections,

$$R(E_i) = \frac{Q_{ion}(E_i)}{Q_{inel}(E_i)} \quad (8)$$

such that, $0 < R \leq 1$

We require $R = 0$ when $E_i \leq I$. This is an exact condition as the ionisation channel opens up only when the incident energy of the projectile is greater than the ionisation threshold of the target implying that the ionisation cross sections will be zero for $E_i \leq I$. The ratio R rises steadily as the energy increases above the threshold, and approaches unity at energies high enough for which the contribution of

the excitation cross sections in Equation (6) becomes negligibly small. We summarise these physical arguments in the form of mathematical equations as,

$$R(E_i) \begin{cases} = 0 & \text{for } E_i \leq I \\ = R_p & \text{at } E_i = E_p \\ \cong 1 & \text{for } E_i \Delta E_p \end{cases} \quad (9)$$

Here, R_p is the value of R at $E_i = E_p$, where E_p stands for the incident energy at which the calculated Q_{inel} attains its maximum value.

Perhaps the first ever estimate of ionisation in relation to the excitation process was made by Turner *et al.* [24]. They conclude from semi-empirical calculations that in gaseous H_2O , ionisation was more probable than excitation above ~ 30 eV. If σ_{ion} and σ_{exc} are the cross sections of the ionisation and excitation, respectively, then above 100 eV,

$$\frac{\sigma_{ion}}{\sigma_{ion} + \sigma_{exc}} \approx 0.75. \quad (10)$$

It should be noted here that the denominator in Equation (10) represents the total inelastic cross sections. This ratio is similar to the ratio defined in this paper vide Equation (8). For a number of stable atoms and molecules like Ne, O_2 , H_2O , CH_4 , SiH_4 , etc., for which the experimental ionisation cross section, Q_{ion} , are known accurately [20,25,26] the general observation is that, at energies close to the peak of ionisation, the contribution of Q_{ion} is about 70–80% of the total inelastic cross sections, Q_{inel} . This behaviour is attributed to the smaller values of $\sum Q_{exc}$ compared to Q_{ion} with increase in energy beyond the peak of inelastic cross sections.

For calculating the Q_{ion} from Q_{inel} we need R in the following manner [23–27]:

$$R(E_i) = 1 - f(U).$$

Here,

$$f(U) = C_1 \left(\frac{C_2}{U+a} + \frac{\ln(U)}{U} \right), \quad (11)$$

where U is the dimensionless variable defined as $U = \frac{E_i}{I}$.

The reason for adopting a particular functional form of $f(U)$ in Equation (11) is as follows. As E_i increases above I , the ratio R increases and approaches 1, since the ionisation contribution rises and the discrete excitation contribution decreases. The discrete excitation cross sections, dominated by dipole transitions, fall off as $\frac{\ln(U)}{U}$ at high energies. Accordingly, the function $f(U)$ must also be proportional to $\frac{\ln(U)}{U}$ in a high range of energy. However, the two-term representation of $f(U)$ given in Equation (11) is more appropriate since the first term in brackets ensures better energy dependence at low and intermediate E_i .

The dimensionless parameters C_1 , C_2 and a , involved in Equation (11) reflect the properties of the target under investigation. The three conditions stated in Equation (9) are used to determine these three parameters. Having obtained Q_{ion} through the complex scattering potential-ionisation contribution (CSP-ic), the summed excitation cross sections $\sum Q_{exc}$ can easily be calculated via Equation (6).

III. Results and discussion

In the present work, we have performed a computation of various total cross sections for electrons interacting with methanethiol in gas phase employing the SCOP and CSP-ic methods. The calculations are carried out using the fixed-nuclei static-exchange-polarisation approximation at the equilibrium geometry of the ground state of CH_3SH . The main goal of the present work is twofold; to provide estimates of electron-driven processes for an industrially relevant but less studied molecule, CH_3SH , and to report for the first time the total elastic as well as total ionisations cross sections vis-à-vis those calculated using the Binary-Encounter-Bethe (BEB) theory [28]. Since there are no ionisation data available, either calculated or measured, for electron scattering with CH_3SH , we have calculated Q_{ion} using the BEB model also that combines the Mott cross sections with the high-energy behaviour of Bethe cross sections [28]. The SCOP formalism could be employed successfully from the threshold of the target to 5000 eV.

We have presented our results in a graphical form through Figures 2–4. For ready reference we report the numerical values of all the calculated cross sections in tabular form. In Table 2 values of the total inelastic cross sections,

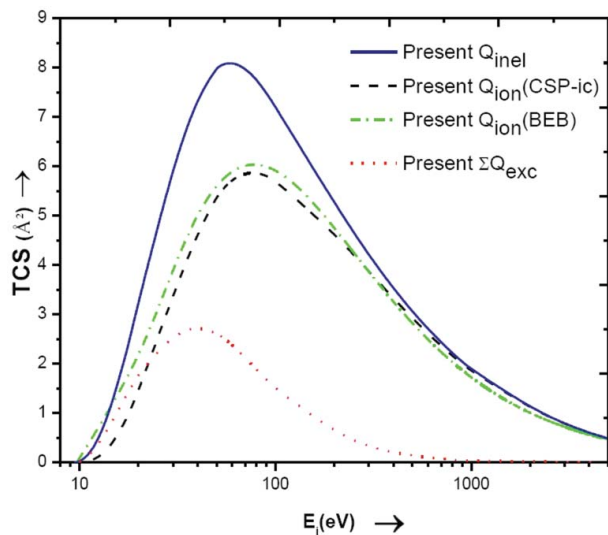


Figure 2. (Colour online) Total inelastic cross sections for e- CH_3SH scattering. Solid line: present Q_{inel} ; dash line: present Q_{ion} (CSP-ic); dash dot line: present Q_{ion} (BEB); dot line: present $\sum Q_{exc}$.

Table 2. Inelastic cross sections (\AA^2).

Energy (eV)	Q_{inel}	Q_{ion}	$\sum Q_{exc}$
10	0.015	0.001	0.014
20	3.237	1.457	1.780
30	6.005	3.390	2.615
40	7.412	4.654	2.758
50	7.983	5.366	2.617
60	8.090	5.713	2.377
70	7.973	5.850	2.123
80	7.754	5.867	1.887
90	7.489	5.813	1.676
100	7.213	5.719	1.494
200	5.252	4.647	0.605
300	4.198	3.874	0.324
400	3.528	3.327	0.201
500	3.059	2.923	0.136
600	2.709	2.612	0.097
700	2.436	2.363	0.073
800	2.218	2.162	0.056
900	2.038	1.993	0.045
1000	1.889	1.853	0.036
2000	1.105	1.097	0.008
3000	0.782	0.779	0.003
4000	0.600	0.598	0.002
5000	0.484	0.483	0.001

viz. Q_{inel} , Q_{ion} and $\sum Q_{exc}$ for energies from the ionisation threshold to 5000 eV are presented. These cross sections are plotted in Figure 2 along with Q_{ion} calculated using the BEB theory. There are no theoretical or experimental data of inelastic cross sections available for comparison for this target.

We have plotted the total inelastic cross sections Q_{inel} with incident electron energy from ionisation threshold through 5000 eV. We have calculated the total ionisation cross sections using two methods, one using CSP-ic method and the other using the BEB formalism. The results using the BEB formalism are slightly higher compared to Q_{ion} calculated using the CSP-ic method, particularly at peak. This feature is expected since as noted by Kim and Rudd [28], the BEB data are accurate within 10% accuracy with experimental results in most cases. This is well reflected in Figure 2. Our present calculations also seek to identify the relative importance of the excitation as against the ionisation in the form of the summed total excitation cross sections. Earlier results on discrete excitation processes reported prior to 1996, have been reviewed by Zecca *et al.* [29]. The lowest curve in Figure 2 shows the summed total excitation cross sections. It is expectedly seen from the figure that the $\sum Q_{exc}$ rises early, attains peak at 40 eV and then falls quickly thereafter as $\ln(E)/E$ for all optically allowed transitions as per the Bethe–Born Approximation [30]. We found a qualitative agreement in the shape of a curve, especially in the peak position, between the quoted results [29] of the sum of all excitation cross sections and the present $\sum Q_{exc}$.

Table 3. Total cross sections (\AA^2).

Energy (eV)	Q_T	Q_{el}
10	41.507	41.492
20	32.398	29.161
30	26.013	20.008
40	21.604	14.192
50	18.984	11.001
60	17.35	9.26
70	16.228	8.255
80	15.382	7.628
90	14.681	7.192
100	14.059	6.846
200	10.406	5.154
300	8.596	4.398
400	7.425	3.897
500	6.576	3.517
600	5.923	3.214
700	5.402	2.966
800	4.978	2.76
900	4.623	2.585
1000	4.328	2.439
2000	2.724	1.619
3000	2.037	1.255
4000	1.644	1.044
5000	1.39	0.906

In Table 3 we have given numerical values of total cross sections Q_T and Q_{el} .

Figure 3 shows the comparison of the present total cross section compared with the lone available experimental data for Q_T reported by Szmytkowski *et al.* [7] from 0.6 eV to 250 eV. No theoretical data are available to the best of our knowledge. The present results of Q_T show excellent agreement with the experimental results of Szmytkowski *et al.* [7] at low energies, below 30 eV. The agreement at

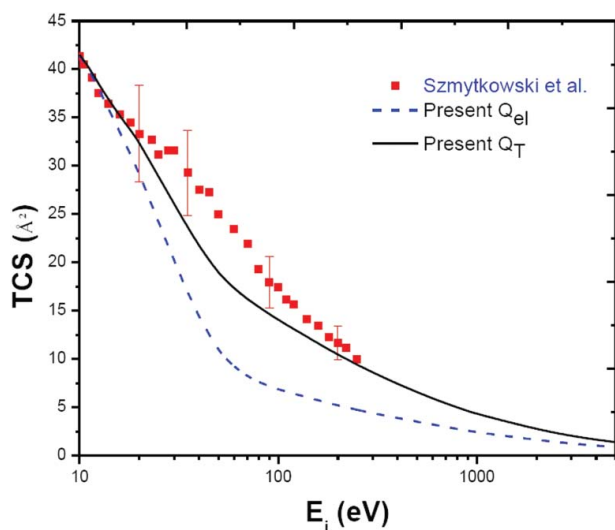


Figure 3. Total cross sections for e-CH₃SH scattering. Solid line: present Q_T ; dash line: present Q_{el} ; squares: Q_T by Szmytkowski *et al.* [7].

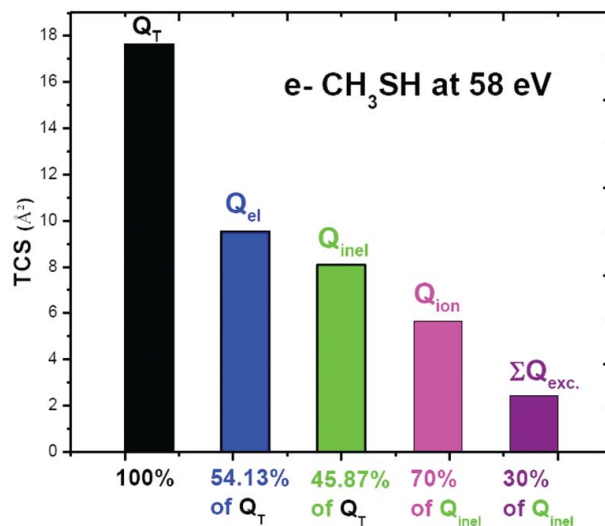


Figure 4. Relative total cross sections for e-CH₃SH at peak of Q_{inel} .

lower energies is important for highly-polar molecules such as methanethiol with a dipole moment of 1.52 D [31] and polarisability of 5.31 \AA^3 [32]. However, between 30 eV and 100 eV present cross sections underestimate the experimental data but are within the quoted uncertainty ($\sim 15\%$) of the experimental data [7]. Beyond 200 eV both results tend to match well. In Figure 3 we have also displayed the present Q_{el} for which no experimental or theoretical data are found.

Figure 4 shows the mutual comparison of various total cross sections for e-CH₃SH scattering at the peak of the total inelastic cross sections, 58 eV. The total (complete) cross sections Q_T , set the upper bound to all cross sections as they include all the scattering processes. The total elastic cross section is 54% of Q_T and the total inelastic cross section is 46% of Q_T . At the peak of the inelastic cross sections, the contribution from total elastic and total inelastic cross sections is equal [33]. In the present case the slight deviation from this is due to the group additivity approximation involved in calculations. The total inelastic cross sections consist of total ionisation and the summed total excitation cross sections. The contribution of total ionisation cross section is about 70% and $\sum Q_{exc}$ is 30% to Q_{inel} . All these cross sections are computed under the single quantum mechanical formalism. This aspect of the present calculation enables relative reliability of the reported data.

IV. Conclusion

The theoretical approach of SCOP along with our CSP-ic method discussed above allows us the determination of various total cross sections Q_T , Q_{el} , and Q_{ion} along with the useful estimation of electronic excitations in terms of the total summed cross section $\sum Q_{exc}$. All these cross sections are computed under the same formalism and hence

render relative reliability for the data. For methanethiol electron interaction studies are scarce and the only cross sections reported are the measured total cross sections from Szymtkowski [7]. For the inelastic processes this industrially as well as biologically relevant molecule is untouched and in this work we have computed Q_{ion} using the CSP-ic as well as the BEB theories and excellent agreement is observed throughout the energy range. In this paper we report for the first time several total cross sections viz. Q_{el} , Q_{inel} , Q_{ion} , and $\sum Q_{exc}$. It is also expected that such efforts will be more appreciated by the research technologies where cross section data are necessary for a further modelling of their systems. We hope that this work would set a reference for further experiments as well as calculations.

Acknowledgements

Chetan Limbachiya thanks UGC, New Delhi, for Major Research Project (F.No. 40-429/2011 (SR)) and Minaxi Vinodkumar thanks the Department of Science and Technology, New Delhi, for Major Research Project Grant No: SR/S2/LOP-26/2008 under which part of this work was done.

References

- [1] M. Hines and M. Morrison, *J. Geophys. Res.* **97**, 16703 (1992).
- [2] Norell, John, Louthan, and P. Rector, "Thiols". *Kirk-Othmer Concise Encyclopedia of Chemical Technology*, 3rd ed. (John Wiley & Sons, Inc., New York, 1988).
- [3] P. Maksymovych, D. Dougherty, X. Zhu, and J. Yates, *PRL* **99**, 016101 (2007).
- [4] K. Jäger and A. Henglein, *Z. Naturf. a* **21**, 1251 (1966).
- [5] D. Amos, R.G. Gillis, J.L. Occolowitzand, and J.F. Pisani, *Org. Mass Spectrom.* **2**, 209 (1969).
- [6] C. Dezarnaud, M. Tronc and A. Modelli, *Chem. Phys.* **156**, 129 (1991).
- [7] C. Szymtkowski, G. Kasperski, and P. Mozejko, *J. Phys. B: At. Mol. Opt. Phys.* **28**, L629 (1995).
- [8] A. Jain, K. Baluja, *Phys. Rev. A* **45**, 202 (1992).
- [9] A. Jain, *Phys. Rev. A* **34**, 3707 (1986).
- [10] A. Jain, *J. Phys. B* **22**, 905 (1988).
- [11] C. Limbachiya, M. Vinodkumar, N. Mason, *Phys. Rev. A* **83**, 042708 (2011).
- [12] H.L. Cox, Jr., and R.A. Bonham, *J. Chem. Phys.* **47**, 2599 (1967).
- [13] S. Hara, *J. Phys. Soc. Japan* **22**, 710 (1967).
- [14] X. Zhang, J. Sun and Y. Liu, *J. Phys. B: At. Mol. Opt. Phys.* **25**, 1893 (1992).
- [15] G. Staszewska, D.W. Schwenke, D. Thirumalai and D.G. Truhlar, *Phys. Rev. A* **28**, 2740 (1983).
- [16] M. Vinodkumar, C. Limbachiya, M. Barot, and N. Mason, *Eur. Phys. J. D* **66**, 74 (2012).
- [17] M. Vinodkumar, C. Limbachiya, and M. Barot, *Mol. Phys.* **110**, 3015 (2012).
- [18] M. Vinodkumar, H. Bhutadia, C. Limbachiya, K. Joshipura, *Int. J. Mass Spectrom.* **308**, 35 (2011).
- [19] M. Vinodkumar, C. Limbachiya, K. Joshipura, and N. Mason, *Eur. Phys. J. D* **61**, 579 (2011).
- [20] F. Blanco and G. Garcia, *Phys. Lett. A* **317**, 458 (2003).
- [21] M. Vinodkumar, C. Limbachiya, and H. Bhutadia, *J. Phys. B: At. Mol. Opt. Phys.* **43**, 015203 (2010).
- [22] M. Rahman, S. Gangopadhyay, C. Limbachiya, K. Joshipura, and E. Krishnakumar, *Int. J. Mass Spectrom.* **319–320**, 48 (2012).
- [23] M. Vinodkumar, K. Korot, and P.C. Vinodkumar, *Eur. Phys. J. D* **59**, 379 (2010).
- [24] J.E. Turner, H.G. Paretzke, R.N. Hamm, H.A. Wright, and R.H. Richie, *Radiat. Res.* **92**, 47 (1982).
- [25] M. Vinodkumar, C. Limbachiya, B. Antony and K.N. Joshipura, *J. Phys. B: At. Mol. Opt. Phys.* **40**, 3259 (2007).
- [26] G.P. Karwasz, R.S. Brusa, and A. Zecca, *Nuovo Cimento*, **24**, 1 (2001).
- [27] M. Vinodkumar, C. Limbachiya, K. Korot, K. Joshipura, and N. Mason, *Int. J. Mass Spectrom.* **273**, 145 (2008).
- [28] Y.K. Kim and M.E. Rudd, *Phys. Rev. A* **50**, 3954 (1994).
- [29] A. Zecca, G.P. Karwasz, and R.S. Brusa, *La Rivista Del Nuovo Cimento* **19**, 1 (1996).
- [30] B.L. Schram, and L. Vriens, *Physica* **31**, 1431 (1965).
- [31] D.R. Lide, *CRC Handbook of Physics and Chemistry*, 74th ed. (Chemical Rubber Company, Boca Raton, FL, 1993–94).
- [32] K.J. Miller, *J. Am. Chem. Soc.* **112**, 8533 (1990).
- [33] C.J. Joachain, *Quantum Collision Theory* (North Holland, Amsterdam, 1983).